Biochemistry

 Volume 29, Number 29 July 24, 1990

Perspectives in Biochemistry

Structural Characteristics of α-Helical Peptide Molecules Containing Aib Residues†

Isabella L. Karle*,‡ and Padmanabhan Balaram§

Laboratory for the Structure of Matter, Naval Research Laboratory, Washington, D.C. 20375-5000, and Molecular Biophysics Unit, Indian Institute of Science, Bangalore 560 012, India

Received March 30, 1990

The α-aminoisobutyryl residue $-NHC(CH_3)_2C(O)-$ (Aib or U), although not one of the 20 amino acid residues found in proteins, is a common residue that occurs in peptides produced by microbial sources. Examples of such peptides that possess antibiotic properties are chlamydocin, a peptide with a cyclic backbone (Closse & Huguenin, 1974; Flippen & Karle, 1976), and linear peptides composed of 15–20 residues such as alamethicin, antiamoebin, emerimicin, and zervamicin (Rinehart et al., 1979) that produce voltage-gated ion channels in lipid membranes (Mueller & Rudin, 1968; Mathew & Balaram, 1983). Each of the linear peptides contains 5–8 Aib residues in addition to L-residues that occur in proteins. The preliminary results of a crystal structure of alamethicin (Fox & Richards, 1982) showed that the 20-residue alamethicin molecule folds into a single helix that is predominantly α-helical. Recently, a published abstract concerning the crystal structure of trichorzianine (Le Bars et al., 1988) reports that its conformation is very similar to that of alamethicin.

The replacement of the proton on the C^α atom in an alanine residue with another methyl group severely restricts the possible rotations about the $N-C^\alpha$ and $C^\alpha-C'$ bonds. The torsion angles about these bonds are designated by ϕ and ψ, respectively. In the manner of Ramachandran et al. (1963, 1968) for calculating allowable ϕ and ψ space, Marshall and Boshard (1972) and Burgess and Leach (1973) showed that the allowable ϕ and ψ angles for the Aib residue occurred in two very restricted regions near −57°, −47° and +57°, +47°. These two regions correspond to a right-handed α-helix or 3_{10}-helix and a left-handed α-helix or 3_{10}-helix, respectively. Since the Aib residue does not have an asymmetric C^α atom, either the L- or D-configuration is equally possible. The handedness of a helix containing Aib residues is fixed by the presence of other residues in the sequence that have the L- or D-handedness.

The implications of the ϕ, ψ map for the Aib residue have indeed been borne out. A review of 28 crystal structures of synthetic tri-, tetra-, and peptapeptides containing at least one Aib residue has shown that all but one contain an incipient 3_{10}-helix (Toniolo et al., 1983). Crystal structure analyses of longer (6–20 residues) Aib-containing peptides, listed in Table I, have shown that these peptides fold into predominantly α-helices, although some have 3_{10}-helices or mixed $3_{10}/\alpha$-helices. Among the very few exceptions to helix formation by the Aib residue are the structure of dihydrochlamydocin (Flippen & Karle, 1976), where the Aib residue is part of an all-trans cyclic tetrapeptide backbone with ω values near 162° instead of 180°, and the structure of

Boc-Cys-Val-Aib-Ala-Leu-Cys-NHMe
(S-S)

where the Aib residue is part of a β-bend in the antiparallel β-hairpin structure (Karle et al., 1988a).

Many of the peptides shown in Table I have been modeled on fragments of the naturally occurring membrane-active peptides. Others have been designed to examine the effects of the positioning of the Aib residue and of special sequences. All are composed of apolar residues and all yield good crystals from various organic solvents by slow evaporation.

The crystals of many of the longer peptides are stable only when surrounded by mother liquor or water and must be mounted in thin glass capillaries for X-ray data collection. Crystals of other similar peptides are quite stable in the dry state. Better diffraction data, with less attenuation of intensity with increasing scattering angle, can often be obtained by cooling the crystal with a stream of liquid nitrogen to ~−70 °C. However, this technique has not always been successful, since some of the peptide crystals shatter upon cooling. X-ray scattering data are usually obtained to resolutions of 0.90 Å

† This research was supported in part by the Office of Naval Research, by National Institutes of Health Grant GM30902, and by a grant from the Department of Science and Technology, India.

‡ Naval Research Laboratory.
§ Indian Institute of Science.

0006-2960/90/0429-6747$02.50/0

Table I: Crystal Structures of Aib-Containing Peptides[a]

No.	Sequence	Helix Type[b]	Reference
Ia)	Ac-Aib-Pro-Aib-Ala-Aib-Ala-Gln-Aib-Val-Aib-Gly-Leu-Aib-Pro-Val-Aib-Aib-Glu-Gln-Pho	A	Fox & Richards 1982
Ib)	Boc- Ala-Aib-Ala-Aib-Ala-Glu(OBzℓ)-Ala-Aib-Ala-Aib-Ala-OMe	A	Bosch et al, 1985a
Ic)	Boc -Leu-Aib-Pro-Val-Aib-Aib-Glu(OBzℓ)-Gln-Pho	A	Bosch et al, 1985b
Id)	Boc-Aib-Pro-Val-Aib-Val-Ala-Aib-Ala-Aib-Aib-OMe	T	Francis et al, 1983
IIa)	Ac-Phe-Aib-Aib-Aib-Val-Gly-Leu-Aib-Aib-OBzℓ	A†	Marshall et al, 1990
IIb)	pBrBz -Aib-Aib-Aib-Val-Gly-Leu-Aib-Aib-OMe	T	Bavoso et al, 1986
IIc)	pBrBz -Aib-Aib-Aib-Aib-Aib-Leu-Aib-Aib-OMe (2 conformers)	T T	Bavoso et al, 1988
IId)	pBrBz -Aib-Aib-Aib-Aib-Leu-Aib-Aib-OMe	T	Bavoso et al, 1988
IIe)	pBrBz -Aib-Aib-Aib-Aib-Aib-Aib-Aib-Aib-OMe	T	Bavoso et al, 1986
IIIa)	Boc-Val-Aib-Val-Aib-Val-Aib-Val-OMe	T	Francis et al 1985
IIIb)	Boc-Aib-Val-Aib-Aib-Val-Val-Val-Aib-Val-Aib-OMe (2 conformers)	A† A/T	Karle et al, 1989a
IIIc)	Boc-Leu-Leu-Leu-Aib-Leu-Leu-Leu-Aib-OBzℓ	A	Okuyama et al, 1988
IIId)	Boc-Val-Val-Aib-Pro-Val-Val-Val-OMe	T	Karle et al, 1990a
IIIe)	Boc-Val-Ala-Leu-Phe-Aib-Val-Ala-Leu-Phe-OMe	A	To be published
IVa)	Boc-Trp-Ile-Ala-Aib-Ile-Val-Aib-Leu-Aib-Pro-Ala-Aib-Pro-Aib-Pro-Phe-OMe	A,T,B	Karle et al, 1987
IVb)	Boc-Trp-Ile-Ala-Aib-Ile-Val-Aib-Leu-Aib-Pro-OMe·$2H_2O$	A†	Karle et al, 1986
IVc)	Boc-Trp-Ile-Ala-Aib-Ile-Val-Aib-Leu-Aib-Pro-OMe·isopropanol	A	Karle et al, 1990b
IVd)	Boc-Trp-Ile-Ala-Aib-Ile-Val-Aib-Leu-Aib-Pro-OMe (anhydrous)	T/A	Karle et al, 1988b
IVe)	Ac-Trp-Ile-Ala-Aib-Ile-Val-Aib-Leu-Aib-Pro-OMe (anhydrous)	A/T	Karle et al, 1990b
Va)	Boc-Val-Ala-Leu-Aib-Val-Ala-Leu-----Val-Ala-Leu-Aib-Val-Ala-Leu-Aib-OMe	A†	Karle et al, 1990c
Vb)	Boc-Val-Ala-Leu-Aib-Val-Ala-Leu-Aib-Val-Ala-Leu-Aib-Val-Ala-Leu-Aib-OMe	A	Karle et al, 1990c
Vc)	Boc -Aib-Val-Ala-Leu-Aib-Val-Ala-Leu-Aib-Val-Ala-Leu-Aib-OMe	A	Karle et al, 1989b
Vd)	Boc -Aib-Val-Ala-Leu-Aib-Val-Ala-Leu-Aib-OMe	A	Karle et al, 1988c
Ve)	Boc -Val-Ala-Leu-Aib-Val-Ala-Leu-Aib-OMe (2 conformers)	A A/T	Karle et al, 1990d
Vf)	Boc -Val-Ala-Leu-Aib-Val-Ala-Leu- OMe (2 conformers)	A A(W)	Karle et al, 1990d
VIa)	Boc-Aib-Ala-Leu-Ala-Leu-Aib-Leu-Ala-Leu-Aib-OMe·isopropanol	A	Karle et al, 1990e
VIb)	Boc-Aib-Ala-Leu-Ala-Leu-Aib-Leu-Ala-Leu-Aib-OMe·methanol	A†	Karle et al, 1990e
VIc)	Boc-Aib-Ala-Leu-Ala-Aib-Aib-Leu-Ala-Leu-Aib-OMe (anhydrous)	A†	Karle et al, 1990f
VId)	Boc-Aib-Ala-Leu-Ala-Aib-Aib-Leu-Ala-Leu-Aib-OMe·isopropanol	A†	Karle et al, 1990g
VIe)	Boc-Aib-Ala-Aib-Ala-Leu-Ala-Leu-Aib-Leu-Aib-OMe (2 conformers)	A† A	Karle et al, 1990f
VIIa)	Boc -Ala-Leu-Aib-Ala-Leu-Aib-OMe	T(W)	Karle et al, 1989c
VIIb)	Boc-Aib-Ala-Leu-Aib-Ala-Leu-Aib-Ala-Leu-Aib-OMe·$2H_2O$·CH_3OH	A(W)	Karle et al, 1988d
VIIc)	Boc-Aib-Ala-Leu-Aib-Ala-Leu-Aib-Ala-Leu-Aib-OMe (anhydrous)(2 conformers)	A† A	To be published

[a] With six or more residues. [b] Helix types: A†, totally α-helix; A, predominantly α-helix; T, 3_{10}-helix; A/T or T/A, mixed $\alpha/3_{10}$-helix; A, T, B, α-, 3_{10}-, and β-ribbon helix; (W), water inserted into backbone.

or better. Anisotropic least-squares refinements result in R factors ranging from 4 to 10% for 2000–9000 carefully measured X-ray intensities. The results of these single-crystal analyses of linear peptides not only establish the precise helical conformation of each crystalline peptide but also provide valuable information on hydrogen bonding, helix aggregation, solvation, and conformational heterogeneity.

The stabilization of helical peptide conformation by incorporation of Aib residues into peptide sequences is a recognized and well-established phenomenon (Balaram, 1984; Prasad & Balaram, 1984; Bosch et al., 1985a; Bavoso et al., 1988; Uma & Balaram, 1989). Crystallization may, in fact, be a consequence of appreciable conformational homogeneity in solution, suggesting that such sequences may be ideal candidates for design and construction of stereochemically rigid modules in a "molecular Meccano (or Lego) set" approach to the synthesis of protein mimics. The use of apolar (hydrophobic) sequences permits characterization of conformations in poorly solvating organic solvents, under conditions where peptide folding is largely controlled by nonbonded interactions, intramolecular hydrogen bonding, and electrostatic effects. Such a situation is less complex and more tractable at the present stage of synthetic design than studies in aqueous solutions, where hydrophobic effects generally play a major but incompletely understood role in dictating the nature of polypeptide folding (Creighton, 1985). Aib-containing sequences have therefore been chosen for the construction of stereochemically rigid helical segments in a modular approach to synthetic protein design (Karle et al., 1989b).

Factors Governing Type of Helix

The conformational preference of Aib-containing peptides has been addressed recently, considering such factors as helix length, the inherent stability of the α-helix as compared to the 3_{10}-helix in long sequences, the additional NH···O=C hydrogen bond in a 3_{10}-helix for the same number of residues, solvent polarity, intermolecular interactions, packing efficiency in crystals, and sequence dependence (Marshall et al., 1990). A significant number of additional crystal structure analyses of longer helical peptides have become available since the preparation of the above paper. Accordingly, additional observations can be made.

Table I contains a list of helical peptides with 6–20 residues whose crystal structures are known presently. They are divided into seven groups, with each group having similar sequences. Those labeled 2 conformers have two independent molecules per asymmetric unit of a unit cell in a crystal. Some others with the same sequence (but not necessarily the same cocrystallized solvent) occur in different crystal forms (polymorphs) with different packing motifs. The helix type denoted by the symbol A^+ indicates a completely α-helical backbone, and A indicates an α-helical backbone except for a 3_{10}-helix-type hydrogen bond at one or both termini. The symbol T indicates a complete 3_{10}-helix, whereas the symbol T/A denotes a mixed $3_{10}/\alpha$-helix. The 16-residue peptide IVa has three Pro residues near the C-terminus, which are involved in three successive β-bends that twist into an approximate 3_{10}-helix. The helix types from Table I for peptides with six residues or more are represented in Figure 1.

Figure 1, showing the distribution of the types of helices with a plot of the total number of residues in a peptide vs the number of Aib residues (the type of helix is indicated by ▲ = T, ● = A, and Ⓐ = T/A), provides a simple graphic delineation between helix type. The 3_{10}-helix is preferred for the shorter peptides ($n \sim 8$ or less), and the α-helix is preferred for the longer peptides (n = 9–20). Furthermore, the presence

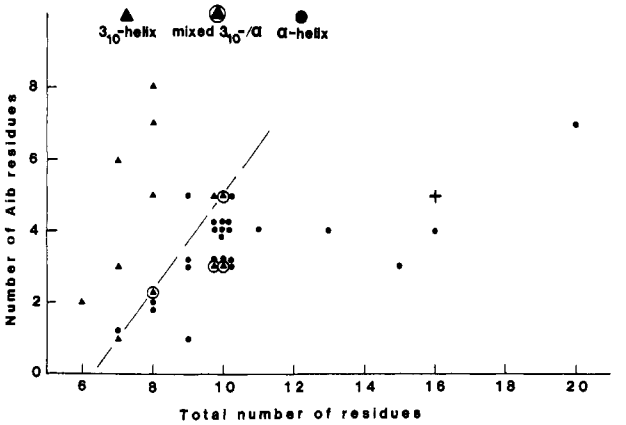

FIGURE 1: Helix type as a function of the total number of residues in peptide and total number of Aib residues. The dashed line separating the 3_{10}-helices from the α-helices has been placed arbitrarily. Peptides containing Aib residues, but with five or fewer total residues, overwhelmingly form a 3_{10}-helix or an incipient 3_{10}-helix and are omitted from the plot. The + symbol indicates a 16-residue, totally helical peptide with three Pro residues.

of a large fraction of Aib residues in a peptide induces a 3_{10}-helix. These results reaffirm the suggestions from earlier observations when fewer structures of the longer peptides were known (Bosch et al., 1985b; Toniolo et al., 1985; Karle et al., 1986).

At the interface between 3_{10}-helices and α-helices in Figure 1, there is some overlap in helix types. For the most part, they are pairs of peptides of the same sequence that undergo a facile $3_{10}/\alpha$ transition when they are crystallized in different polymorphs or when they occur in the same crystal with more than one independent molecule (i.e., not related by crystal symmetry). For example, the structure of Boc-Trp-Ile-Ala-Aib-Ile-Val-Aib-Leu-Aib-Pro-OMe (IVb–e in Table I and points at 3 Aib/10 residues in Figure 1) has been analyzed in four different crystal forms, with different cocrystallized solvents or a different end group (Ac replacing Boc) (Karle et al., 1986, 1988b, 1990b). In crystals IVb and IVc, both in space group $P1$ with parallel packing of helices, the helix is the α-type, except for the helix reversal at Aib,[9] which occurs relatively often at an Aib residue if it is in an ultimate position or occasionally in the penultimate position. In crystal IVd, in space group $P2_1$ with parallel packing, the helix has switched to a primarily 3_{10}-type with only two 5→1-type hydrogen bonds in the middle. Figure 2 shows a superposition of the two helix types with the predominantly 3_{10}-helix being longer than the predominantly α-helix. In crystal IVe, where the Boc end group has been replaced by Ac, the helices pack in an antiparallel fashion in space group $P2_1$. In this crystal, there is one 3_{10}-type hydrogen bond in the middle of the α-helix. Usually in mixed $3_{10}/\alpha$-helices, the 3_{10}-type hydrogen bonds are only at the termini. The $3_{10}/\alpha$-helix transitions in this group of four polymorphs cannot be ascribed to the differences in environment between parallel and antiparallel packing of helices nor to differences evolving from the exchange of Ac and Boc end groups at the N-terminus. The cocrystallized solvents, or lack thereof, do change the environment of the peptides somewhat and may contribute to the helix transitions.

In the second case of $3_{10}/\alpha$-helix transitions in the same peptide, Boc-(Val-Ala-Leu-Aib)$_2$-OMe (Ve in Table I and points at 2 Aib/8 residues in Figure 1), the two helices alternate in the same crystal. One helix is completely α-helical; the other is mixed with three 4→1-type hydrogen bonds interspersed with three 5→1 hydrogen bonds (Karle et al., 1990d). Similarly, in the crystal of Boc-Aib-Val-Aib-Aib-Val-Val-Val-Aib-Val-Aib-OMe (IIIb in Table I and points

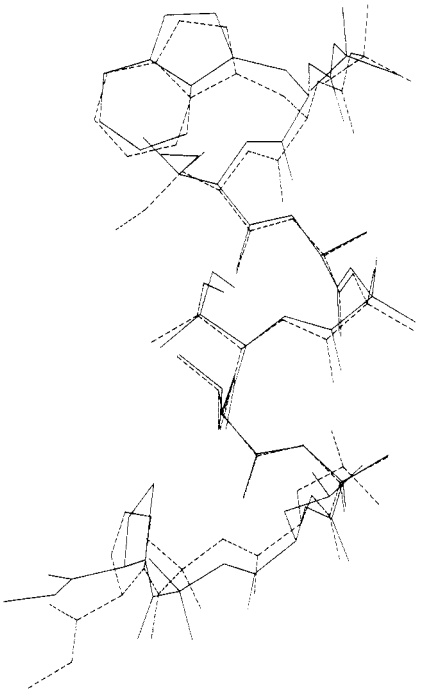

FIGURE 2: Superposition (with a least-squares fit of the backbone atoms) of Boc-Trp-Ile-Ala-Aib-Ile-Val-Aib-Leu-Aib-Pro-OMe in two different crystal forms, solid line in space group $P2_1$ (Karle et al., 1988b) and dashed line in space group $P1$ (Karle et al., 1986). The backbone of the conformer shown by the dashed line is predominantly α-helical, while the backbone in the conformer shown by the solid line has only two α-helical-type hydrogen bonds near the middle and the remainder at both ends are the 3_{10}-helix type.

at 5 Aib/10 residues in Figure 1), one helix that is completely α-helical alternates with another that has 3_{10}-helical segments at either end plus an unwinding of the backbone at the N-terminus. Figure 3 shows a superposition of the two conformers (Karle et al., 1989a). In these cases, the crystallizing conditions are identical since only one crystal is involved. Finally, the completely α-helical Ac-Phe-Aib-Aib-Aib-Val-Gly-Leu-Aib-Aib-OBzl (IIa and points at 5 Aib/9 residues in Figure 1) (Marshall et al., 1990) occupies a somewhat anomalous position in Figure 1, considering the high Aib content. Previous experience suggests that a different polymorph of this peptide could have a mixed $3_{10}/\alpha$-helix. An explanation for the easy $3_{10}/\alpha$ transitions in different molecules of the same peptide, as well as the partial unwinding of the backbone, as in Figure 3, must rest on the near equality of the stability of the two forms and on other factors concerning subtle changes in environment that are not well understood.

Number of Aib Residues

The question of how many Aib residues are needed to induce helix formation in longer peptides has been answered partially by the structures of three peptides: Boc-Val-Val-Aib-Pro-Val-Val-Val-OMe, IIId (Karle et al., 1990a); Boc-Val-Ala-Leu-Aib-Val-Ala-Leu, Vf (Karle et al., 1990d); and Boc-Val-Ala-Leu-Phe-Aib-Val-Ala-Leu-Phe-OMe, IIIe (to be published). These hepta- and nonapeptides have only one Aib residue, located in the middle in each sequence. The first peptide forms a 3_{10}-helix, and the latter two are predominantly α-helical. The high propensity of Aib for helix formation is demonstrated particularly by peptide IIId, in which one Aib residue overcomes the effects of five Val residues and one Pro residue, which are known to be poor helix formers (Chou & Fasman, 1974). The longest sequence of non-Aib residues in a helix, among the known structures, occurs as a string of six residues in the middle of Boc-Val-Ala-Leu-Aib-*Val-Ala-Leu-Val-Ala-Leu*-Aib-Val-Ala-Leu-Aib-OMe, Va (Karle et al., 1990c). This peptide is completely α-helical, as shown in Figure 4.

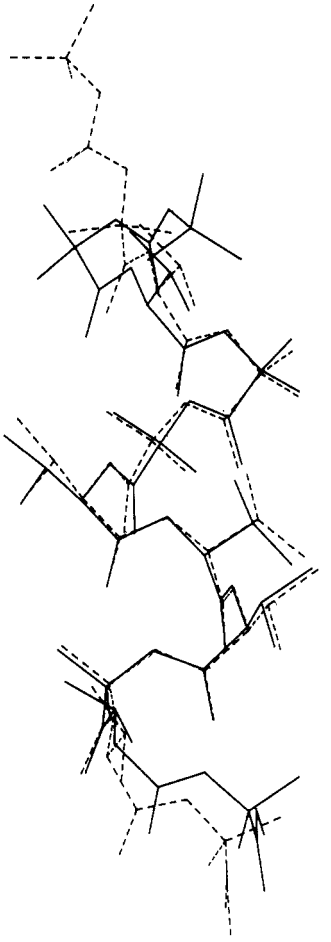

FIGURE 3: Superposition of the two conformers of Boc-Aib-Val-Aib-Aib-Val-Val-Val-Aib-Val-Aib-OMe occurring side by side in the same crystal. The conformer shown by the solid line is completely α-helical. The one shown by the dashed line has 3_{10}-type hydrogen bonds at both ends plus an unwinding of the backbone at the N-terminus (Karle et al., 1989a).

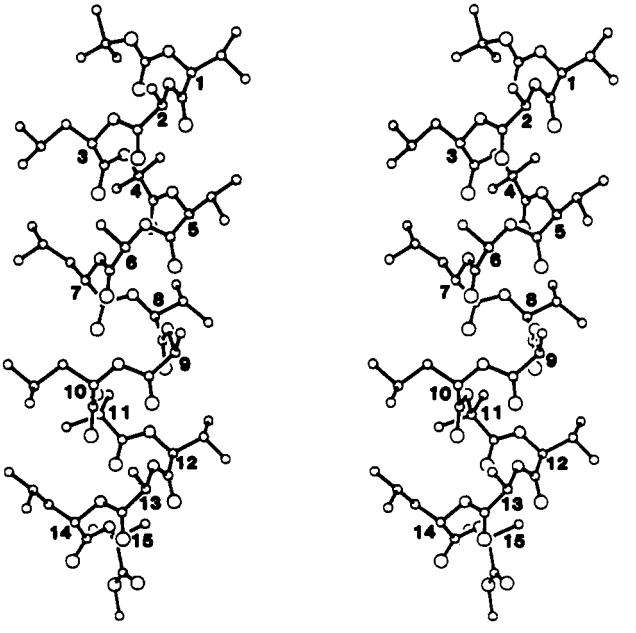

FIGURE 4: Stereo diagram of completely α-helical Boc-Val-Ala-Leu-Aib-Val-Ala-Leu-Val-Ala-Leu-Aib-Val-Ala-Leu-Aib-OMe (Karle et al., 1990c). This helical peptide contains six contiguous non-Aib residues.

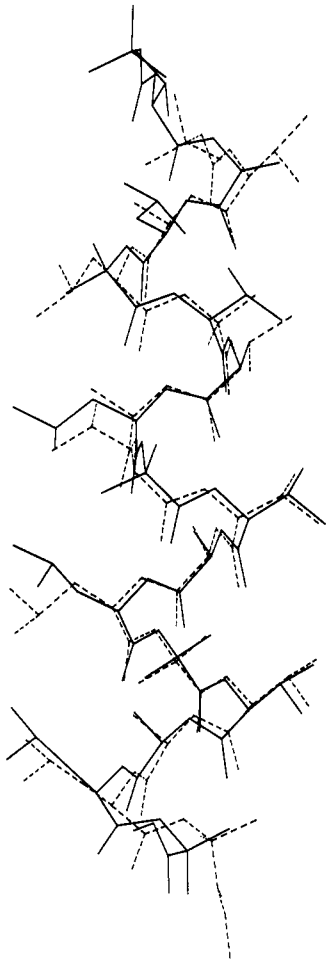

FIGURE 5: A superposition of Boc-(Val-Ala-Leu-Aib)$_4$-OMe (solid line) and the 15-residue peptide with Aib^8 deleted (dashed line, also shown in Figure 4). The sequence of the last eight residues is the same, and the sequence in the top half has a shift of one due to the omission of Aib^8 from the 15-residue peptide; nevertheless, the helical nature of the backbone is almost undisturbed (Karle et al., 1990c).

Position of Aib Residue in Sequence

Two series of peptides were designed and analyzed to evaluate the effects of the presence of Aib residues at the C- or N-termini of a sequence, the removal of Aib from the middle of a sequence, and the exchange of Aib with Leu or Ala residues. In the first series, Va–f in Table I, 7–16-residue peptides were synthesized by using the tetrad (Val-Ala-Leu-Aib)$_n$ with Aib residues added or removed. In the second series, VIa–e and VIIa–c in Table I, 6- and 10-residue peptides were synthesized by using the triad (Ala-Leu-Aib)$_n$, or permutations of Ala, Leu, and Aib, with Aib added to the N-terminus of the peptide.

The 15-residue peptide Va differs from the 16-residue peptide Vb only by the deletion of Aib^8 from the middle of Vb. The helical structure of the backbones in the two peptides is entirely similar. A least-squares fit of backbone atoms N(3)–O(14) in Vb with N(2)–O(13) in Va yields a rms deviation of 0.28 Å. A superposition of the two molecules is shown in Figure 5, where the final eight residues are the same but the initial residues are shifted by one because of the deletion of the middle Aib in Va (Karle et al., 1990c).

The decapeptides VIa and VIc differ only by the exchange of Leu^5 in VIa by Aib^5 in VIc. The effect of such a replacement on conformation is minuscule. The rms deviation of the backbone atoms in the two peptides is only 0.12 Å (Karle et al., 1990f). The isomeric decapeptides VIc and VIe differ by the interchange of Leu and Aib at residues 3 and 5 and the interchange of Ala and Aib at residues 6 and 8. Even with changes at four sites, the conformations of the two peptides are very similar, with a rms deviation of only 0.26 Å for the backbone atoms (Karle et al., 1990f). The conclusion that can be drawn from these structure analyses is that an Aib residue can replace an apolar residue, or vice versa, without disturbing the α-helix. The precise positioning of Aib residues in these cases is without effect on the α-helical nature of the backbone.

All but two of the 18 peptides in groups V, VI, and VII, as well as several others in Table I, terminate with a Leu-Aib-OMe sequence; peptides Id and IIa–e terminate with an Aib-Aib-OMe (or OBzl) sequence and two others with an Ala-Aib-OMe sequence. Only in three of the peptides does the terminal Aib residue continue the right-handed helix with ϕ and ψ values near −54° and −47°, respectively. In 14 of the peptide molecules there is a helix reversal at the final Aib residue to a left-handed helix with ϕ and ψ values near +54° and +45°, respectively. The helix reversal at the final Aib residue had already been noted in the 2–5-residue peptides (Toniolo et al., 1983). However, another conformation for the terminal Aib residue appeared in some of the longer peptides. The final Aib residue is semiextended with ϕ and ψ values near −57° and +150°, respectively, in peptides Va, Vc, and VIa, near −57° and +180° in peptides Vd, Ve, and VIb, and near +57° and −150° in peptide VIIb. Conformational energy maps for the Aib residue (Marshall, 1972; Burgess & Leach, 1973; Uma & Balaram, 1989) do show minor elongated minima in the ϕ, ψ space corresponding to the observed ϕ and ψ values.

The presence or absence of an Aib residue at the N-terminus does not appear to affect the helical nature of peptides; see, e.g., peptides Va–f.

The Spread of ϕ, ψ Conformational Angles for α-Helices

The torsional angles ϕ (torsion about the N–C$^\alpha$ bond) and ψ (torsion about the C$^\alpha$–N bond) have been plotted in a Ramachandran-type plot in Figure 6 for each residue separately for the helical peptides in groups VI and VII in Table I, which contain only Aib, Ala, and Leu residues, and for helical peptides in group V, which contain Aib, Ala, Val, and Leu residues, in panels a and b, respectively. The values for the Aib residues at the C-terminus have been omitted because of the helix reversal that occurs often. A previous plot, using a different choice of peptide helices (Karle et al., 1990f), separated only the Aib residues from the remainder. In both the previous plot and the plots in Figure 6, the ϕ and ψ values for Aib (●) occur in a concentrated region near −55° and −45°, respectively (at the right-hand side of the distribution), a region that coincides with the original calculations of conformational energy maps for the Aib residue. In the present maps, the ϕ and ψ values for individual residues are plotted separately for each to determine whether the large spread in the observed ϕ and ψ values is a function of the type of residue. The clusters of points for the Ala residue (+) are much larger than those for Aib. In both panels a and b, the center of the Ala clusters is near −65° and −35°. In Figure 6b, the cluster for the Val residues (/) is longer than that for Ala residues (along the diagonal direction where ϕ and ψ are related inversely), and the center of the cluster appears to have moved to the left slightly with ϕ and ψ near −67° and −35°. Finally, the distribution for the Leu residues (▲) not only overlaps the distributions for Ala and Val but also extends far to the left with some points at $\phi < -100°$. Many of the Leu residues that fall on the far left in the distribution are the penultimate residue

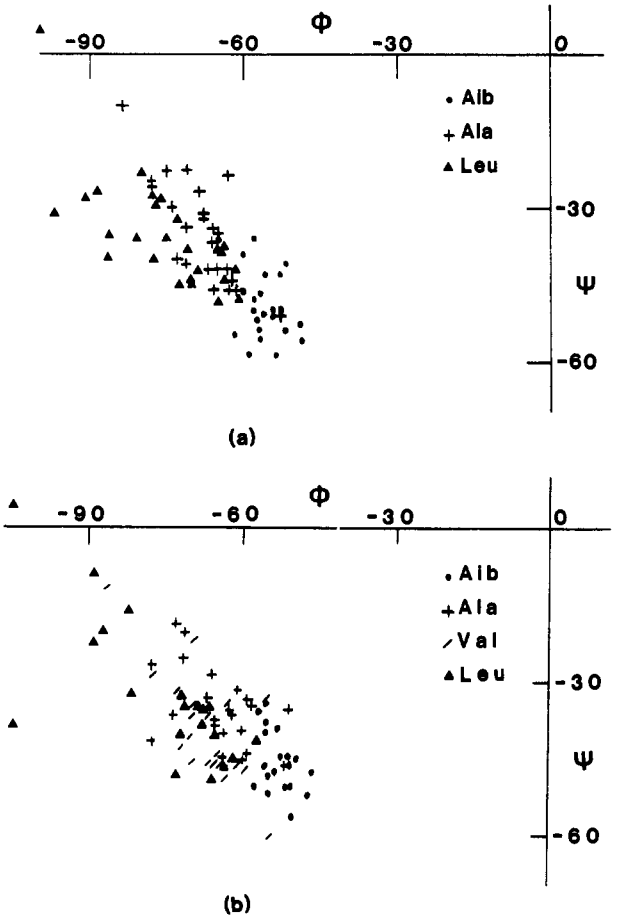

FIGURE 6: Observed torsional angles in right-handed α-helices of Aib-containing peptides where ϕ is the rotation about the N–C^{α} bond and ψ is the rotation about the C^{α}–C′ bond. (a) Data from crystal structures of decapeptides containing Aib, Ala, and Leu residues in various sequences. (b) Data from crystal structures of 7–16-residue peptides containing the tetrad $(Val\text{-}Ala\text{-}Leu\text{-}Aib)_n$ and the addition or deletion of Aib residues.

in the peptide sequence and followed by an Aib that reverses the helix direction. However, other Leu residues with aberrant ϕ and ψ values occur in the middle of a peptide sequence. The wide range of ϕ and ψ values actually observed is larger than previously anticipated. Furthermore, there is a suggestive dependence upon type and/or size of residue, since the clusters of observed ϕ and ψ values in α-helices increase in spread and move leftward and upward in Figure 6 for the Ala, Val, and Leu residues, respectively.

Hydrogen Bonds

5→1 Hydrogen Bond in α-Helix. The spread of ϕ and ψ angles, discussed above, contributes to minor irregularities in the α-helix. These irregularities are manifested primarily by the spread of N···O distances in the 5→1 hydrogen bonds. Criteria for accepting a 5→1 hydrogen bond (or choosing between a 4→1 and a 5→1 hydrogen bond in a distorted helix) include not only the N···O distance but also the NH···O distance and the direction of the NH bond toward the O atom (with the NH···O angle 150°–180°). The distribution of the N···O distances in 5→1 hydrogen bonds in peptides IIIb, IVa–c, Va–f, VIa–e, and VIIb–c from Table I is shown in Figure 7b. There is a continuous distribution from 2.89 to 3.25 Å, with several outliers on either side and a median value of 3.06 Å. A plot of C=O···N angles for the same 5→1 hydrogen bonds, Figure 7c, is approximately Gaussian with a median value of 156°. Plots of N···O distances and C=O···N angles in 12 α-helices of refined proteins (resolution 2.0 Å or

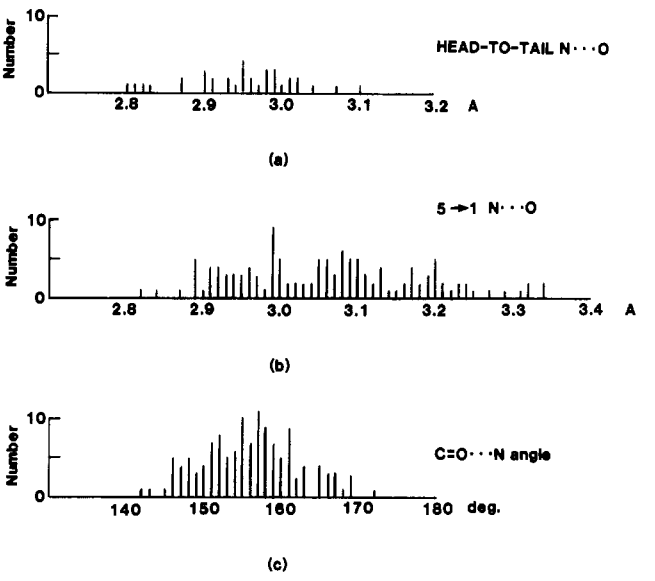

FIGURE 7: Observed values of hydrogen bonds in α-helices of Aib-containing peptides. (a) Distribution of N···O distance values in hydrogen bonds between helices. (b) Distribution of N···O distance values in 5→1-type hydrogen bonds in α-helices. (c) Distribution of C=O···N angle values in α-helix-type hydrogen bonds.

better) indicate about the same median value for the angle and a somewhat smaller median value for the N···O distance, ~3.00 Å (Barlow & Thornton, 1988), although the spread of N···O values is quite comparable for α-helices in proteins and in Aib-containing helical peptides.

Head-to-Tail Hydrogen Bonds. All the peptides listed in Table I form continuous rods in crystals by head-to-tail hydrogen bonding. Since almost all the side chains in these peptides are hydrocarbons (except for group I in Table I), there are no direct lateral hydrogen bonds between helices. In an isolated ideal α-helix, N(1)H, N(2)H, and N(3)H at the top of the helix, with the NH moieties directed upward, and C=O(f), C=O(f − 1), and C=O(f − 2) (where f is the final residue at the bottom of the helix), with all C=O moieties directed downward, do not participate in the intramolecular 5→1 hydrogen bonds. These NH and C=O moieties participate in head-to-tail hydrogen bonds in various modes: (a) It is possible to form three direct NH···O=C hydrogen bonds in perfect register, as illustrated by peptide IIIb in Figure 8a. (b) Two direct NH···O=C bonds may be formed by utilizing N(1)H and N(2)H, while N(3)H remains unsatisfied. The head-to-tail region of peptide VIe is shown in Figure 8b. The nearest atom in any neighboring molecule to N(3) is O(10) at 3.9 Å. It is not unusual for an N(2)H or N(3)H moiety not to participate in any hydrogen bonding owing to a lack of acceptor. Inefficient crystal packing appears to be the cause. (c) There may be only one direct NH···O=C hydrogen bond and the remaining head-to-tail hydrogen bonds are mediated by several water molecules, as shown by the 15-residue peptide Va in Figure 8c. (d) There are no direct NH···O=C hydrogen bonds in peptide IVd in Figure 8d. Rather, the NH in a side chain of the first residue (Trp) forms a bifurcated hydrogen bond with two carbonyl oxygens from the upper molecule, and the OH of a 2-propanol solvent molecule mediates hydrogen bonding between N(1)H and O(7) of the upper molecule. A 4→1 type of hydrogen bond is formed between N(3)H···O(0), where O(0) is part of the Boc end group. Further, N(2)H remains unsatisfied. The closest atom in any neighboring molecule to N(2) is O(10) (in the upper molecule) at 5.5 Å.

The above examples show the adaptability of helical peptides, even with end groups present, to a variety of head-to-tail

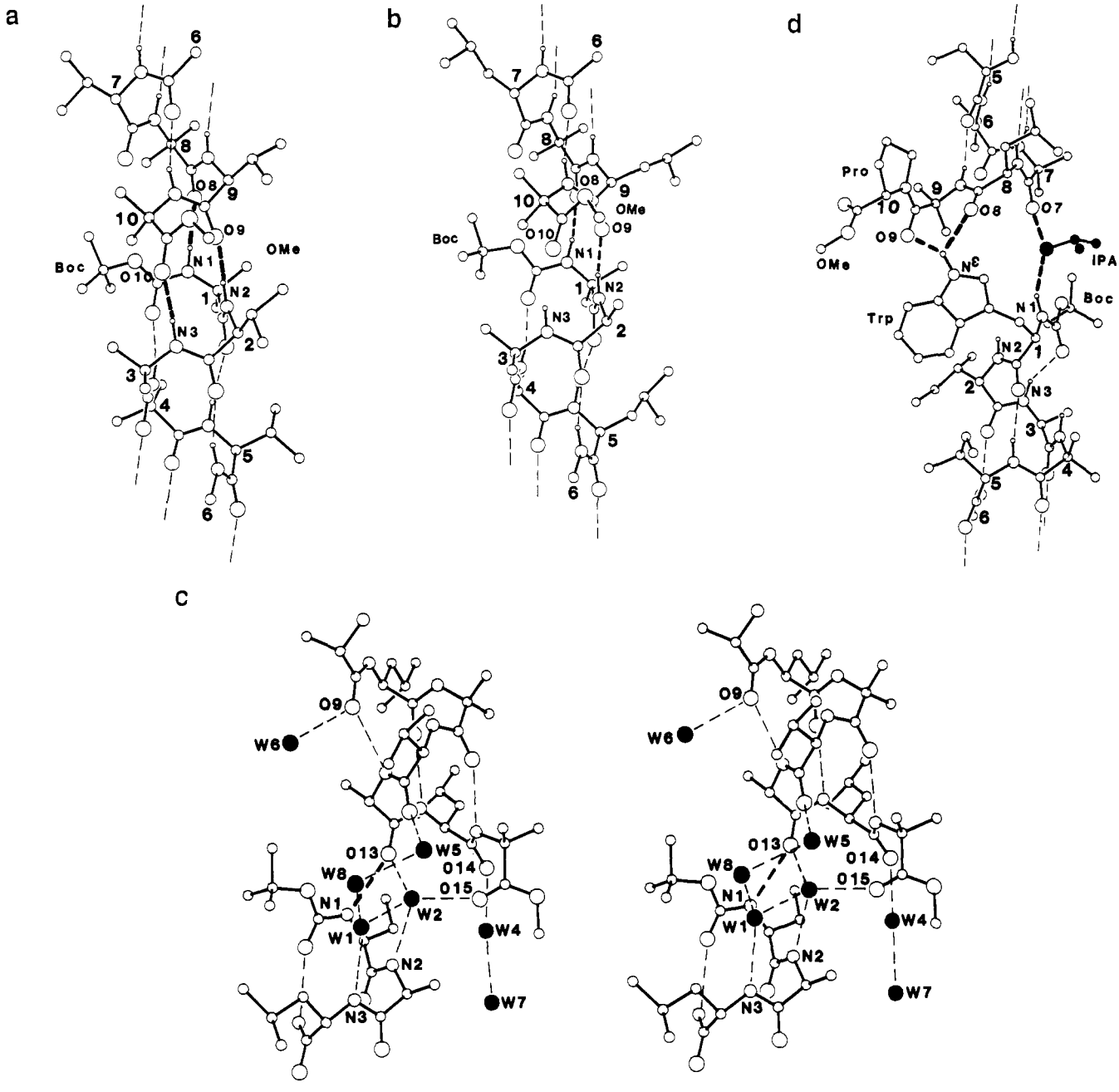

FIGURE 8: Modes of head-to-tail hydrogen bonding between helices. The lower part of one helical molecule is shown over the upper part of a neighboring helical molecule. The head-to-tail hydrogen bonds are emphasized by heavy dashed lines. (a) Three direct intermolecular NH···O=C bonds in perfect register in peptide IIIb (Karle et al., 1989a). (b) Two direct NH···O=C bonds in peptide VIe. The N(3)H moiety does not participate in any hydrogen bonding (Karle et al., 1990f). (c) One direct N(1)H···O(13) bond in peptide Va. Water W(2) mediates hydrogen bonds between N(2)H and O(13) and O(15). Water molecules W(1), W(8), and W(5) mediate hydrogen-bond connections between N(3)H and O(12) (Karle et al., 1990c). A stereo diagram is shown. (d) No direct NH···O=C backbone head-to-tail hydrogen bonds in peptide IVc. The NH in the Trp side chain makes a bifurcated hydrogen bond to O(8) and O(9). The OH in 2-propanol mediates hydrogen bonds between N(1) and O(7). The N(2)H moiety does not participate in any hydrogen bonding (Karle et al., 1989b).

hydrogen-bonding schemes. The distribution of N···O distances in direct head-to-tail bonding is shown in Figure 7a, where the median N···O distance is 2.95 Å.

Water in Hydrophobic Helical Structures

An example of the intimate association of water with hydrophobic α-helices has been demonstrated in the head-to-tail hydrogen-bonding region (Figure 8c). Both ends of the α-helices or 3_{10}-helices are quite polar around the extended NH and CO moieties that are free to form direct NH···O=C hydrogen bonds between helices or hydrogen bonds mediated by water molecules (or alcohol molecules). The occurrence of water near the middle of helices where the apolar side chains create an apparently totally hydrophobic environment is more unusual. Three different modes of hydration have been found among Aib-containing helical peptides.

Exposed Carbonyls. The presence of a Pro residue in the middle of a sequence that forms a helix results in the loss of an intramolecular hydrogen bond due to the lack of a proton on the N in the Pro. The bulk of the pyrrolidine ring causes the helix to bend ~30° and exposes the free C=O group at the bend to the outside environment. The 16-residue apolar peptide IVa affords such an example, in which the bend in the helix caused by Pro^{10} results in the extension of $C=O^7$ away from the nearby hydrocarbon side chains from Leu and Aib. The $C=O^7$ attracts a water molecule, which in turn makes a hydrogen bond to another water molecule, resulting in a minipolar area on the hydrophobic helix (Karle et al., 1987).

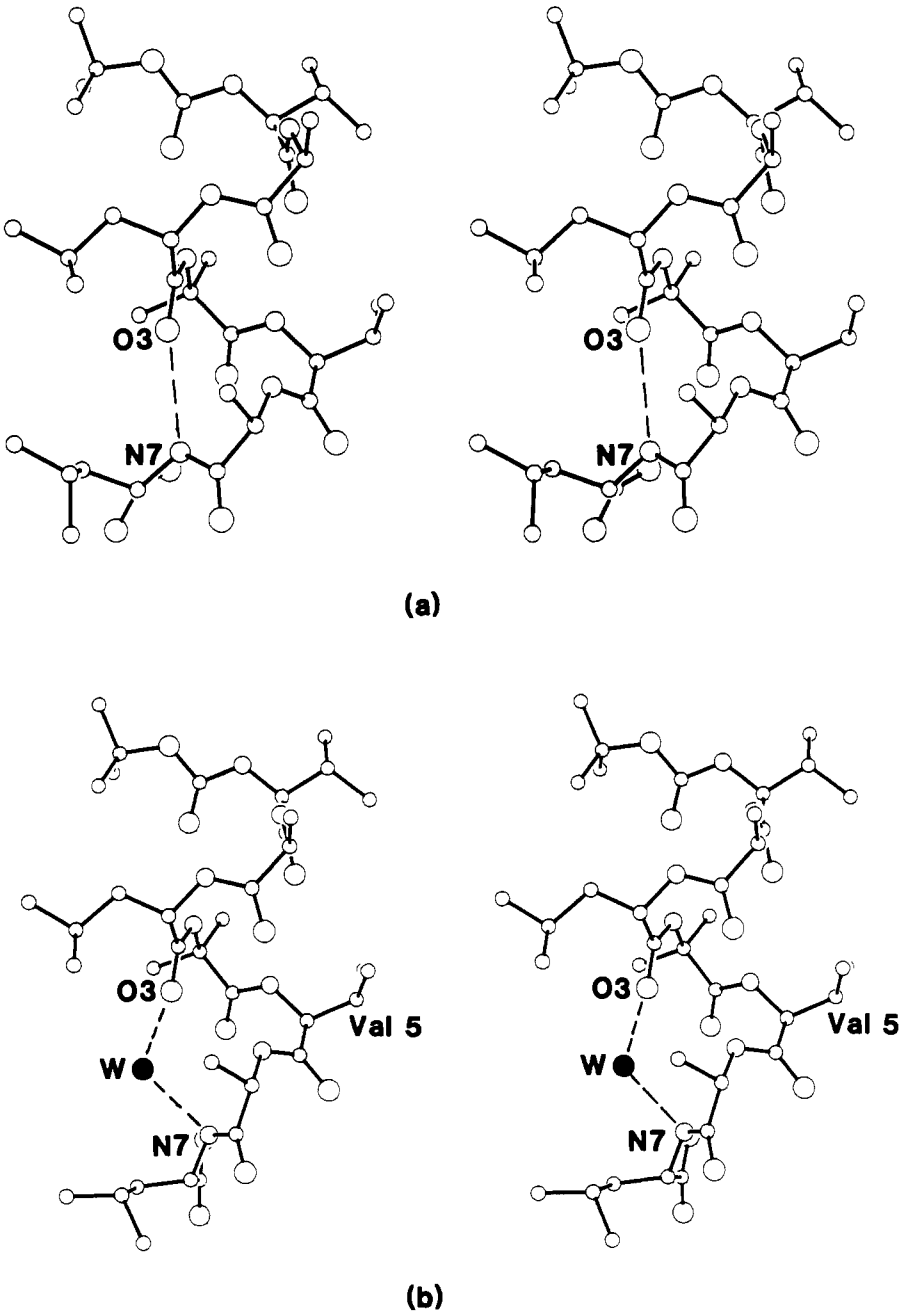

FIGURE 9: Stereo diagrams of two peptide molecules that occur side by side in a crystal of Vf. (a) The backbone is in the form of a normal helix. (b) The N(7)H···O(3) hydrogen has been broken by the insertion of a water molecule W. Two new hydrogen bonds have been formed, W···O(3) and N(7)H···W (Karle et al., 1990d).

Bifurcated 5→1 Hydrogen Bonds. The side chains in apolar helices often pack in an inefficient manner in a crystal lattice, leaving voids predominantly surrounded by hydrophobic moieties. These voids can be occupied by water molecules that make a hydrogen bond to a carbonyl group in the helix that is already involved in a 5→1 hydrogen bond. Such bifurcated hydrogen bonds involving water molecules (or 2-propanol) have been observed in the apolar peptides Va, Vc, Vd, VIc, and VIe. In peptides Vc and VIe, a water molecule links neighboring helices by hydrogen bonds to carbonyl oxygens and may be instrumental in stabilizing the structure, which otherwise lacks the possibility for any lateral hydrogen bonds (Karle et al., 1989b). Similar bifurcated hydrogen bonds in proteins between helix and water or a side-chain group have been reported and analyzed (Blundell et al., 1983; Barlow & Thornton, 1988; Sundaralingam & Sekharudu, 1989). In proteins, such bifurcated bonds generally occur in polar rather than in apolar environments. A notable exception occurs in the structure of the photosynthetic reaction center of the purple bacterium *Rhodopseudomonas viridis*, where a water molecule cross-links two hydrophobic transmembrane helices by forming hydrogen bonds with carbonyl oxygens that also are involved in α-helix hydrogen bonds (Deisenhofer & Michel, 1989).

Water Insertion into Backbone. The most interesting mode of hydration is that of a rupture of a 5→1 hydrogen bond in a helix and the spreading of the NH and CO moieties to incorporate a water molecule into the helix backbone. In peptide Vf (Karle et al., 1990d) there are two independent peptide molecules side by side in the crystal. One peptide molecule is totally helical (Figure 9a). In the other peptide molecule, the α-helical N(3)···O(7) hydrogen bond has been severed by the entry of water molecule W, which in turn makes two new hydrogen bonds, W···O(3) and N(7)···W, 2.77 and 2.97 Å, respectively. The opening of the helix has been accomplished by a minimum of motion, that is, by ϕ and ψ rotations at $C^{\alpha}(5)$ of Val^5, −87°, −11° before hydration and

-91°, +2° after hydration. None of the other torsional angles has been changed significantly. It should be noted that, except for the hydrogen bonds, the water molecule is entirely surrounded by hydrophobic side chains of its own molecule as well as from neighboring molecules.

Another example of a very similar insertion of water into a helix is afforded by the hydrophobic peptide VIIb (Karle et al., 1988d) and its anhydrous polymorph VIIc. In this case, the normal helix for VIIc and the hydrated helix for VIIb occur in different crystals grown from ethylene glycol and methanol/water, respectively. The opening of the helix to accommodate the water molecule occurs at Leu[3] with major changes of ϕ and ψ values from -75°, -42° for the normal helix to -102°, +15 for the hydrated helix. Contrary to the predominantly hydrophobic environment for the water in the peptide in Figure 9, peptide VIIb acquires amphiphilic character by the insertion of water into the helix and subsequent attraction of additional water (Karle et al., 1988d). The six-residue peptide VIIa (a fragment of VIIb) also has a water molecule inserted into the helix in a mode identical with that of VIIb (Karle et al., 1989c).

The occurrence of both the normal helix and internally hydrated helix next to each other in the same crystal of Vf and in polymorphs VIIb and VIIc grown in the same manner (but with a different solvent) points to the facile transformation between the unhydrated and hydrated helices and to the probable role of water in helix folding.

Similar water insertion into the helix of troponin C (Satyshur et al., 1988) prompted a search that identified an additional 19 proteins with internally hydrated helices (Sundaralingam & Sekharudu, 1989c).

Implications for Peptide Design

The crystal structures of Aib-containing peptides described in this paper establish that stable helical conformations, predominantly or totally α-helical, can be maintained in 10–16-residue peptides containing triads, tetrads, and even hexads of non-Aib residues. Helical rods having three to more than four turns of $3_{10}/\alpha$-helix can be readily constructed. The precise positioning of Aib residues, or their total number, appears to be without effect on the backbone. The helical conformation of diverse sequences, with 10–50% Aib residues, suggests that stable helical segments can be constructed reproducibly and that Aib can be substituted for other residues to promote helix formation. Such segments can provide an important element in a modular approach to synthetic protein design, as, for example, in piecing together a hydrophobic four-helix bundle.

Acknowledgments

We are deeply indebted to our colleagues K. Uma and M. Sukumar (India) and Judith L. Flippen-Anderson (Washington) for their crucial contributions to the investigations reviewed here.

Registry No. Aib, 62-57-7.

References

Balaram, P. (1984) *Proc.—Indian Acad. Sci. 93*, 703–717.

Barlow, D. J., & Thornton, J. M. (1988) *J. Mol. Biol. 201*, 601–619.

Bavoso, A., Benedetti, E., Di Blasio, B., Pavone, V., Pedone, C., Toniolo, C., & Bonora, G. M. (1986) *Proc. Natl. Acad. Sci. U.S.A. 83*, 1988–1992.

Bavoso, A., Benedetti, E., Di Blasio, B., Pavone, V., Pedone, C., Toniolo, C., Bonora, G. M., Formaggio, F., & Crisma, M. (1988) *J. Biomol. Struct. Dyn. 5*, 803–817.

Blundell, T. L., Barlow, T. J., Borkakoti, N., & Thornton, J. M. (1983) *Nature (London) 306*, 281–283.

Bosch, R., Jung, G., Schmitt, H., & Winter, W. (1985a) *Biopolymers 24*, 961–978.

Bosch, R., Jung, G., Schmitt, H., & Winter, W. (1985b) *Biopolymers 24*, 979–999.

Burgess, A. W., & Leach, S. J. (1973) *Biopolymers 12*, 2599–2605.

Chou, P. Y., & Fasman, G. D. (1974) *Biochemistry 13*, 222–245.

Closse, A., & Huguenin, R. (1974) *Helv. Chim. Acta 57*, 533–545.

Creighton, T. E. (1985) *J. Phys. Chem. 89*, 2452–2459.

Deisenhofer, J., & Michel, H. (1989) *EMBO J. 8*, 2149–2170.

Flippen, J. L., & Karle, I. L. (1976) *Biopolymers 15*, 1081–1092.

Fox, R. O., Jr., & Richards, F. M. (1982) *Nature (London) 300*, 325–330.

Francis, A. K., Iqbal, M., Balaram, P., & Vijayan, M. (1983) *FEBS Lett. 155*, 230–232.

Francis, A. K., Vijayakumar, E. K. S., Balaram, P., & Vijayan, M. (1985) *Int. J. Pept. Protein Res. 26*, 214–223.

Karle, I. L., Sukumar, M., & Balaram, P. (1986) *Proc. Natl. Acad. Sci. U.S.A. 83*, 9284–9288.

Karle, I. L., Flippen-Anderson, J. L., Sukumar, M., & Balaram, P. (1987) *Proc. Natl. Acad. Sci. U.S.A. 84*, 5087–5091.

Karle, I. L., Kishore, R., Raghothama, S., & Balaram, P. (1988a) *J. Am. Chem. Soc. 110*, 1958–1963.

Karle, I. L., Flippen-Anderson, J. L., Sukumar, M., & Balaram, P. (1988b) *Int. J. Pept. Protein Res. 31*, 567–576.

Karle, I. L., Flippen-Anderson, J. L., Uma, K., & Balaram, P. (1988c) *Int. J. Pept. Protein Res. 32*, 536–543.

Karle, I. L., Flippen-Anderson, J. L., Uma, K., & Balaram, P. (1988d) *Proc. Natl. Acad. Sci. U.S.A. 85*, 299–303.

Karle, I. L., Flippen-Anderson, J. L., Uma, K., Balaram, H., & Balaram, P. (1989a) *Proc. Natl. Acad. Sci. U.S.A. 86*, 765–769.

Karle, I. L., Flippen-Anderson, J. L., Uma, K., & Balaram, P. (1989b) *Biochemistry 28*, 6696–6701.

Karle, I. L., Flippen-Anderson, J. L., Uma, K., & Balaram, P. (1989c) *Biopolymers 28*, 773–781.

Karle, I. L., Flippen-Anderson, J. L., Uma, K., Balaram, H., & Balaram, P. (1990a) *Biopolymers* (in press).

Karle, I. L., Flippen-Anderson, J. L., Sukumar, M., & Balaram, P. (1990b) *Int. J. Pept. Protein Res.* (in press).

Karle, I. L., Flippen-Anderson, J. L., Uma, K., & Balaram, P. (1990c) (submitted for publication).

Karle, I. L., Flippen-Anderson, J. L., Uma, K., & Balaram, P. (1990d) *Proteins: Struct., Funct., Genet. 7*, 62–73.

Karle, I. L., Flippen-Anderson, J. L., Uma, K., & Balaram, P. (1990e) *Biopolymers* (in press).

Karle, I. L., Flippen-Anderson, J. L., Uma, K., & Balaram, P. (1990f) *Biopolymers* (in press).

Karle, I. L., Flippen-Anderson, J. L., Uma, K., & Balaram, P. (1990g) *Curr. Sci.* (submitted for publication).

Le Bars, M., Bachet, B., & Mornon, J. O. (1988) *Z. Kristallogr. 185*, 588.

Marshall, G. R., & Bosshard, H. E. (1972) *Circ. Res. 30/31 (Suppl. II)*, 143–150.

Marshall, G. R., Hodgkin, E. E., Langs, D. A., Smith, G. D., Zabrocki, J., & Leplawy, M. T. (1990) *Proc. Natl. Acad. Sci. U.S.A. 87*, 487–491.

Mathew, M. K., & Balaram, P. (1983) *Mol. Cell. Biochem. 50*, 47–64.

Mueller, P., & Rudin, D. O. (1968) *Nature (London) 217*, 713-719.
Okuyama, K., Tanaka, N., Doi, M., & Narita, M. (1988) *Bull. Chem. Soc. Jpn. 61*, 3115-3120.
Prasad, B. V. V., & Balaram, P. (1984) *CRC Crit. Rev. Biochem. 16*, 307-348.
Ramachandran, G. N., & Sasisekharan, V. (1968) *Adv. Protein Chem. 23*, 284-437.
Ramachandran, G. N., Ramakrishnan, C., & Sasisekharan, V. (1963) *J. Mol. Biol. 7*, 95-99.
Rinehart, K. L., Jr., Pandey, R. C., Moore, M. L., Tarbox, S. R., Snelling, C. R., Cook, J. C., Jr., & Milberg, R. H. (1979) in *Peptides. Proceedings of the Sixth American Peptide Symposium* (Gross, E., & Meienhofer, J., Eds.) pp 59-71, Pierce Chemical Co., Rockford, IL.
Satyshur, K. A., Rao, S. T., Pyzalska, D., Drendel, W., Greaser, M., & Sundaralingam, M. (1988) *J. Biol. Chem. 263*, 1628-1647.
Sundaralingam, M., & Sekharudu, Y. C. (1989) *Science 244*, 1333-1337.
Toniolo, C., Bonora, G. M., Bavoso, A., Benedetti, E., Di Blasio, B., Pavone, V., & Pedone, C. (1983) *Biopolymers 22*, 205-215.
Toniolo, C., Bonora, G. M., Bavoso, A., Benedetti, E., Di Blasio, B., Pavone, V., & Pedone, C. (1985) *J. Biomol. Struct. Dyn. 3*, 585-598.
Uma, K., & Balaram, P. (1989) *Indian J. Chem. 28B*, 705-710.

Accelerated Publications

Contribution of Exogenous Substrates to Acetyl Coenzyme A: Measurement by ^{13}C NMR under Non-Steady-State Conditions†

Craig R. Malloy,*,‡,§ Jennifer R. Thompson,‖ F. Mark H. Jeffrey,§ and A. Dean Sherry‖

Department of Internal Medicine, Molecular Cardiology Division, and Department of Radiology, University of Texas Southwestern Medical Center at Dallas, 5323 Harry Hines Boulevard, Dallas, Texas 75235-8573, and Department of Chemistry, University of Texas at Dallas, Richardson, Texas 75083-0688

Received April 24, 1990; Revised Manuscript Received May 22, 1990

ABSTRACT: A method is presented for the rapid determination of substrate selection in a manner that is not restricted to conditions of metabolic and isotopic steady state. Competition between several substrates can be assessed directly and continuously in a single experiment, allowing the effect of interventions to be studied. It is shown that a single proton-decoupled ^{13}C NMR spectrum of glutamate provides a direct measure of the contribution of exogenous ^{13}C-labeled substrates to acetyl-CoA without measurement of oxygen consumption and that steady-state conditions need not apply. Two sets of experiments were performed: one in which a metabolic steady state but a non-steady-state ^{13}C distribution was achieved and another in which both metabolism and labeling were not at steady state. In the first group, isolated rat hearts were supplied with [1,2-^{13}C]acetate, [3-^{13}C]lactate, and unlabeled glucose. ^{13}C NMR spectra of extracts from hearts perfused under identical conditions for 5 or 30 min were compared. In spite of significant differences in the spectra, the measured contributions of acetate, lactate, and unlabeled sources to acetyl-CoA were the same. In the second set of experiments, the same group of labeled substrates was used in a regional ischemia model in isolated rabbit hearts to show regional differences in substrate utilization under both metabolic and isotopic non steady state. This sensitive probe of substrate selection was also demonstrated in intact hearts where excellent time resolution (3 min) of substrate selection was feasible. Since the basis of the method involves measurement of two resonance areas (C4 and C3) and the relative multiplet components of the carbon 4 resonance, simple *J*-modulated editing schemes allow substrate selection to be measured even when ^{13}C–^{13}C coupling cannot be resolved, as would be expected in vivo. The time resolution of these measurements may not be limited by technical contraints but by the rate of carbon flux in the citric acid cycle. Although this technique is demonstrated for the heart, it is applicable to all tissues.

The contribution of exogenous substrates to acetyl-CoA is an important aspect of myocardial energetics and has been an objective of numerous studies (Williamson & Krebs, 1961; Williamson, 1962; Neely et al., 1972; Mickle et al., 1986; Myears et al., 1987; Liedtke et al., 1988, Wyns et al., 1989). Measurement of the respiratory fuel requires an estimate of the rate of acetyl-CoA utilization, typically from oxygen consumption, and the rate of substrate utilization under steady-state conditions. The latter usually is measured by the rate of appearance of $^{14}CO_2$ from a ^{14}C-enriched substrate, the rate of removal of substrate from the perfusion medium, or multiexponential analysis of ^{11}C time–activity curves. However, substrate and oxygen removal are difficult to

† Supported by a Research Associate Award and Merit Review from the Department of Veterans Affairs, NIH HL34557, and the Meadows Foundation.
* Author to whom correspondence should be addressed.
‡ Department of Internal Medicine, University of Texas Southwestern Medical Center at Dallas.
§ Department of Radiology, University of Texas Southwestern Medical Center at Dallas.
‖ Department of Chemistry, University of Texas at Dallas.

0006-2960/90/0429-6756$02.50/0